

## ORIGINAL RESEARCH

# Predictive power of remote sensing versus temperature-derived variables in modelling phenology of herbivorous insects

Juha Pöyry<sup>1</sup> , Kristin Böttcher<sup>1</sup>, Stefan Fronzek<sup>1</sup>, Nadine Gobron<sup>2</sup>, Reima Leinonen<sup>3</sup>, Sari Metsämäki<sup>1</sup> & Raimo Virkkala<sup>1</sup>

<sup>1</sup>Finnish Environment Institute (SYKE), P.O. Box 140, Helsinki, FI-00251, Finland

<sup>2</sup>European Commission Joint Research Centre, Directorate D Sustainable Resources, Via E. Fermi 2749, TP 440, Ispra (VA) 210207, Italy

<sup>3</sup>Kainuu Centre for Economic Development, Transport and the Environment, P.O. Box 115, Kajaani FI-87101, Finland

## Keywords

Modelling, moths, phenology, remote sensing data, spatial prediction, thermal sum

## Correspondence

Juha Pöyry, Finnish Environment Institute (SYKE), Natural Environment Centre, P.O. Box 140, FI-00251 Helsinki, Finland. Tel: +358 295 251534; Fax: +358 9 5490 2390; E-mail: juha.poyry@ymparisto.fi

Editor: Nathalie Pettorelli  
Associate Editor: Kate He

Received: 7 April 2017; Revised: 16 June 2017; Accepted: 20 June 2017

doi: 10.1002/rse2.56

## Abstract

Application of remote sensing datasets in modelling phenology of heterotrophic animals has received little attention. In this work, we compare the predictive power of remote sensing versus temperature-derived variables in modelling peak flight periods of herbivorous insects, as exemplified by nocturnal moths. Moth phenology observations consisted of weekly observations of five focal moth species (*Orthosia gothica*, *Ectropis crepuscularia*, *Cabera exanthemata*, *Dystrota citrata* and *Operophtera brumata*) gathered in a national moth monitoring scheme in Finland. These species were common and widespread and had peak flight periods in different seasons. Temperature-derived data were represented by weekly accumulating growing degree days (GDD) calculated from gridded temperature observations. Remote sensing data were obtained from three sources: (1) snow melt-off date from the MODIS daily snow maps, (2) greening date using the NDWI from MODIS data and (3) dates of start, maximum and end of growing season based on the JRC FAPAR products. Peak phenology observations of moths were related to different explanatory variables by using linear mixed effect models (LMM), with 70% of the data randomly selected for model calibration. Predictive power of models was tested using the remaining 30% of the data. Remote sensing data (snow melt-off and vegetation greening date) showed the highest predictive power in two moth species flying in the early and late spring, whereas in the three other species none of the variables showed reasonable predictive power. Flight period of the spring species coincides with natural events such as snow melt or vegetation greening that can easily be observed using remote sensing techniques. We demonstrate the applicability of our methodology by predictive spatial maps of peak flight phenology covering the entire Finland for two of the focal species. The methods are applicable in situations that require spatial predictions of animal activity, such as the management of populations of insect pest species.

## Introduction

Remote sensing data have been used to observe vegetation phenology (White et al. 2009; Ganguly et al. 2010; Gonsamo and Chen 2016; Vrieling et al. 2017) or the amount of annual net primary productivity across continents (Myneni et al. 1997; Running et al. 2004; Liu et al. 2013),

and their change over time (Ivits et al. 2012; Zhang et al., 2014; Zhao et al. 2015). While modelling of the phenology of plants and vegetation has utilized both temperature-derived and remote sensing data, modelling the phenology of animals has typically relied on using temperature-derived measures such as growing degree days as predictor variables (e.g. Roy et al. 2001; Nietschke et al.

2007; Hodgson et al. 2011), but very few studies have used remote sensing data. By contrast, most studies combining animals and remote sensing data have focused on predicting species occurrence in space (Leyequien et al. 2007; Pettorelli et al. 2011, 2014), with only some exceptions focusing on temporal occurrence of insect abundance (Jepsen et al. 2009a; Trierweiler et al. 2013; Sweet et al. 2015; Olsson et al. 2016).

Several different satellite-based remote sensing indices have been developed and used in studies of vegetation phenology in recent years. These include the Normalized Difference Vegetation Index (NDVI) (Badeck et al. 2004; Karlsen et al. 2006; White and Nemani 2006; Pettorelli et al. 2011), the Normalized Difference Water Index (NDWI) (Delbart et al. 2005, 2008) and the Fraction of Absorbed Photosynthetically Active Radiation (FAPAR) (Verstraete et al. 2008). Thus, it is now possible to explore if such variables could be used in addition to temperature-derived variables to model phenology of animals. Developing such methodologies is also timely as they will support the global targets of conserving biodiversity set by the Convention of Biological Diversity at the Aichi conference (CBD, 2014; O'Connor et al. 2015). One of these targets is development of novel methods for monitoring phenology of terrestrial ecosystems. Therefore, novel initiatives of using earth observation techniques in monitoring changes in ecosystems, including phenology of animal species, at both regional and global scales are urgently needed (e.g. Lausch et al. 2016; Vihervaara et al. 2017).

In this study we test if the phenology of heterotrophic animals, as exemplified by nocturnal moths, can be modelled using remote sensing variables and temperature-derived variables (growing degree days), and compare the predictive power of models fitted using different sets of variables. Firstly, we are particularly interested in understanding under what circumstances do models based on remote sensing data show reasonable power in predicting insect phenology and how they compare to models using variables derived from temperature observations. Secondly, and building on the first aim, we derive predictive spatial models that can be used as phenological indicators to describe the seasonal progress of flight periods of herbivorous insects. As the focal group we selected nocturnal moths, for which we use an extensive monitoring dataset collected between 1993 and 2012 across one country, Finland. Moths comprise a particularly suitable species group for a comparison of predictive power between remote sensing and temperature-derived measures, as they are widespread and abundant enough to allow collecting phenological observations across large geographic areas by using standard methods.

## Materials and Methods

### Study area

The study area covers the total land area of Finland (338 400 km<sup>2</sup>), which largely belongs to the boreal forest zone, with some deciduous-dominated forests in the southern parts of the country. Forests dominate the landscape throughout the country all the way to the very northern parts, which are characterized by subarctic tundra and open bogs. Agricultural areas are concentrated in the south-western parts. Finland's climate is intermediate, combining characteristics of both a maritime and a continental climate. According to Köppen's climate classification most of Finland belongs to the subarctic (or boreal) climate zone (Dfc), whereas the southernmost parts of the country are situated in the warm-summer humid continental zone (Dfb). Snow cover typically covers the whole country, arriving in October–December, melting in April–June, depending on the year. In mild winters the southern parts of the country may lack a continuous seasonal snow cover.

### Moth phenology data

The observations of moth phenology gathered through the Finnish national moth monitoring scheme (Nocturna) constitute the basic phenology data in this work (Leinonen et al. 2016). Moths are observed using light traps that are equipped with Hg bulbs and run every night from the early spring to the late autumn, typically between April and October. The traps are usually emptied weekly and the moth specimens identified by voluntary observers. During the period 1993–2012, altogether 208 trap sites were included in the monitoring network (Leinonen et al. 2016). Of these sites, 51 traps with the least temporal gaps and altogether consisting of 810 trapping years with continuous moth observations were selected for data extraction (Fig. S1).

The focal moth species were selected for phenology modelling based on the following criteria: wide distributional area, high abundance and timing of the peak flight period spread in different parts of the season. The selected five focal species are: *Orthosia gothica* (family Noctuidae, peak flight in late April–early May), *Ectropis crepuscularia* (Geometridae, late May–early June), *Cabera exanthemata* (Geometridae, late June–early July), *Dysstroma citrata* (Geometridae, mid-August) and *Operophtera brumata* (Geometridae, late September–early October). Stages of life cycle of the five focal species in relation to the phenological events detected using remote sensing methods and used in this work are presented in Figure 1. Of the five focal species, *O. brumata* has been subject to considerable research as the species is a forest pest in parts of its range, whereas the four other species have been subject to very few or no

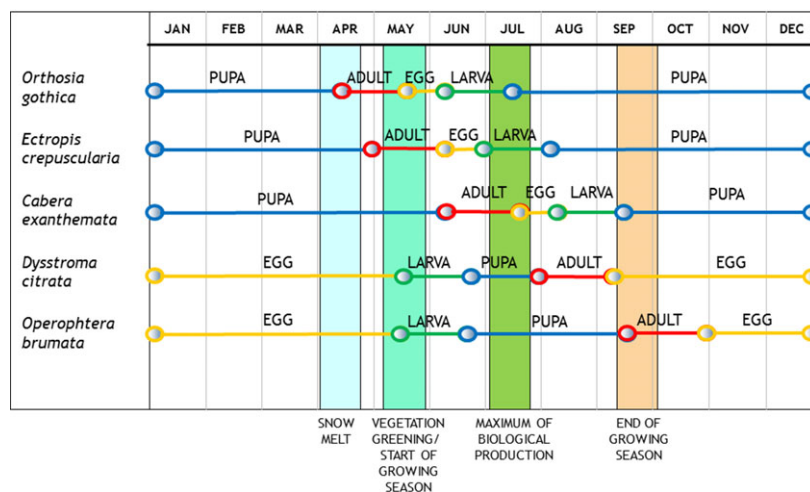


**Figure 1.** Annual life cycle of the five focal moth species (*Orthosia gothica*, *Ectropis crepuscularia*, *Cabera exanthemata*, *Dysstroma citrata* and *Operophtera brumata*) and timing of natural phenomena observed with remote sensing and used in this work. The figure represents a typical phenological sequence during an average year in the southern part of Finland.

ecological studies at all. In *O. brumata*, timing of egg hatching and larval development have been topics of studies due to their high importance to population growth rate and development of defoliations (Jepsen et al. 2009b; van Asch et al. 2013). The nomenclature of moths follows Aarvik et al. (2017).

Peak flights were selected to represent timing of the flight periods because they are less affected by inter-annual abundance variation than other descriptors of the flight period such as start, end and length (e.g. Roy and Sparks 2000). This is because the length of a species' flight period may appear longer in years of high abundance compared to years of low abundance. Peak flights were calculated based on the median occurrence of individuals per year and trap site. Mid-day of the median observation period was used as the peak flight date. Although moth traps are typically emptied weekly, there is some variation in the lengths of observational periods for logistic reasons. Therefore, inaccuracy (expressed as the average length of observational period divided by two) in the mid-day values of the peak flight periods varies slightly across the focal species (due to slight variations in the length of the observational period): *Orthosia gothica* ( $\pm 3.83$  days), *Ectropis crepuscularia* ( $\pm 3.67$  days), *Cabera exanthemata* ( $\pm 3.81$  days), *Dysstroma citrata* ( $\pm 3.85$  days) and *Operophtera brumata* ( $\pm 4.26$  days).

## Explanatory variables

### Geographical variables

Location of each trap site is represented by the latitudinal coordinate of the Finnish national uniform grid system in

metres (YKJ) to account for a potential latitudinal trend in timing of the peak flight. Two of the five focal species (*Orthosia gothica* and *Operophtera brumata*) showed a marked latitudinal gradient in timing of their peak flight period (Fig. S2a, S2e).

### Climatic variables

Time series of daily mean temperatures for the grid cells containing the moths trap locations were extracted from daily gridded temperature dataset in 10 km  $\times$  10 km resolution (Venäläinen et al. 2005; updated). If the location of a moth trap was exactly on the edge between two 10-km grid cells, the cell to the east and north of that point was used. Accumulated temperature sums (growing degree days, GDD) above a base temperature were calculated for the locations of moth traps for each year of the period 1993 to 2012. A total of 18 different summation periods were calculated, all starting on 1 January of each year and ending between 1 April (or 31 March in leap years) and 29 July (28 July in leap years) in weekly intervals. GDDs were calculated using 16 different base temperatures between  $-5^{\circ}\text{C}$  and  $10^{\circ}\text{C}$  with intervals of one degree. This range of base temperatures was selected because previous empirical and modelling studies on insect phenology have shown that the base temperature of accumulated temperature sum affecting adult phenology varies at least from  $-5^{\circ}\text{C}$  to  $10^{\circ}\text{C}$  (Pritchard et al. 1996; Valtonen et al. 2011). This resulted in 288 different GDD indices (16 base temperature times 18 summation periods).

Previous modelling studies focusing on moth phenology that included the focal species of our work have

reported variable base temperatures used in calculations of the temperature sums. For example, Valtonen et al. (2011) reported the base temperatures of  $-5^{\circ}\text{C}$  and  $2^{\circ}\text{C}$  for *Dysstroma citrata* and *Orthosia gothica*, respectively. By contrast, Valtonen et al. (2014) reported the following base temperatures:  $-5.8^{\circ}\text{C}$  and  $-6.0^{\circ}\text{C}$  for *Orthosia gothica*,  $1.9^{\circ}\text{C}$  and  $2.4^{\circ}\text{C}$  for *Ectropis crepuscularia*, and  $3.2^{\circ}\text{C}$  for *Cabera exanthemata*. Thus, base temperatures that produce the best model fit vary from model to model and are also dependent on what variables are included in the model.

### Remote sensing variables

Three kinds of remote sensing products were used in the phenology modelling:

- (1) Date of snow melt in spring was derived for each trap site from time series of daily Pan-European Fractional Snow Cover (FSC) products from CryoLand (Copernicus Service Snow and Land Ice, <http://www.cryoland.eu/>), available for the years 2001–2016 (Nagler et al. 2015). A particular method for extraction of melt-off day despite the gaps in the FSC time series (due to cloudiness that prevent the observations) was developed at the Finnish Environment Institute (SYKE) (Metsämäki et al. 2017). The actual method for FSC retrieval from satellite imagery (NASA Terra/MODIS, Moderate Resolution Imaging Spectroradiometer, in the case of CryoLand) was also developed at SYKE (Metsämäki et al. 2005, 2012), and complemented by a latitude-dependent adjustment related to snow-free ground detection rules within the CryoLand project. Temporal resolution of the snow melt date is 1 day, but days missing due to cloudiness cause some uncertainty in the estimate. Our investigations covering CryoL and FSC time series and the corresponding in situ observations on snow depth for 2001–2016 show that for Finland the mean absolute difference (melt-off day based on FSC–melt-off day from in situ) is less than 5 days, with bias of  $\sim 2.7$  days. The positive bias indicates that CryoLand FSC-based melt-off day is slightly overestimated (i.e. delayed) compared to the in situ-observed melt-off day, the latter indicated by the first day of 0 cm snow depth starting the snow-free season.
- (2) We selected the NDWI for the determination of the greening date of deciduous species in Finland because its detection from NDVI can be affected by snow melt in boreal areas (Moulin et al. 1997; Delbart et al. 2006). Instead, the NDWI decreases during snow melt and increases during the greening up (Delbart et al. 2005), and thus the effect of snow on the observed greening date can be reduced. The date of

greening of the vegetation in Finland was determined from MODIS-derived time series of the NDWI following the method of Delbart et al. (2005) and further described in Böttcher et al. (2016). The greening date was calculated for MODIS pixels with vegetation cover. The vegetation cover per MODIS pixel was estimated from the national CORINE Land Cover 2006 raster product with a spatial resolution of 25 m provided by the Finnish Environment Institute (2009). We took into account all vegetated land cover types. Both understory growth and canopy phenology contribute to the land surface greening observed from the NDWI. Their respective contributions depend on canopy closure, sun and view angles and understory type. At a southern boreal site in Finland the contribution of the understory reflectance was below 30% in the near infrared at the beginning of the growing season in May for different stand types (Rautiainen and Lukes 2015). The vegetation development in spring in boreal forests Finland occurs during a very short time interval and there is no mismatch in the seasonal development of understory and the forest canopy (Rautiainen et al. 2011). The resolution of the greening date maps is  $0.05^{\circ} \times 0.05^{\circ}$ . Temporal resolution of the NDWI is 1 day, but days missing due to cloudiness cause some uncertainty in the estimate of the greening date. For years 2001–2012, depending on the location, in average 34–73% of daily observations were missing during the period of April–July. The greening date was then extracted in the satellite map from the closest pixel to the trap site. These data are available for the years 2001–2012. The greening date in deciduous forests shows good correspondence (RMSE 1 week) with the date of birch bud break in Finland (Böttcher et al. 2016).

- (3) Fraction of Absorbed Photosynthetically Active Radiation (FAPAR)-derived dates of start (FSGS), peak (FMD) and end (FEGS) of growing season were acquired from the Joint Research Centre (JRC) datasets (Gobron et al. 2006; Jung et al. 2008; Ceccherini et al. 2013b, 2014), and extracted at each trap site. The FAPAR used in this study covers the period from January 1998 to December 2012 using harmonized SeaWiFS and MERIS datasets with a nominal spatial resolution of 1.5 km (Gobron et al. 2006; Ceccherini et al. 2013a). The FAPAR values correspond to the 10-day time composite products spatially averaged over  $3 \times 3$  pixels around the trap sites for FSGS and FEGS. For FMD, FAPAR values were derived for the pixel overlapping with the trap site.

Examples of timing of the peak flight periods of the focal moth species, snow melt-off dates (SMD), vegetation greening dates derived from the NDWI and dates of

**Table 1.** The number of peak flight observations in the selected 51 sites and across the five focal species with different limitations of data.

Species	Total number of flight period observations in 1993–2012	Number of peak flight observations in 1993–2012	Peak flight observations in 2003–2011 with remote sensing data
<i>Orthosia gothica</i>	3644	790	282
<i>Ectropis crepuscularia</i>	2291	608	220
<i>Cabera exanthemata</i>	4176	704	231
<i>Dysstroma citrata</i>	5890	829	520
<i>Operophtera brumata</i>	2130	709	449

FAPAR start (FSGS), peak (FMD) and end (FEGS) of the growing season are presented in Figure S3. In order to compare the predictive power of models built using different variables, datasets of moth phenology, climatic variables and remote sensing variables were combined for the period 2003–2011. The impact of data availability on the amount of peak flight observations in the five focal species is shown in Table 1. Cross-correlations among the explanatory variables in all five focal species are shown in Table S1.

## Modelling methods

An overview of datasets used and analysis steps conducted for deriving predictive models of moth phenology is presented in Figure 2. Details of modelling methods are described in the following paragraphs.

### Comparing predictive power of different variables

Peak flight dates of each focal moth species were related to explanatory variables using linear mixed effect models (LMM) (Venables and Ripley 2002). Explanatory variables tested for all focal species included latitude and thermal sum (GDD), whereas the inclusion of remote sensing variables differed depending on timing of the peak flight period of the species in question (Table 2). A single GDD index for each species was selected by minimizing the value for the Akaike Information Criterion (AIC; Burnham and Anderson 2002) in univariate LMMs of the 288 GDD indices as explanatory variable.

The performance of LMMs was evaluated for both total models including all explanatory variables and for univariate models, that is, models including one variable at a time.

This was done in order to determine the proportion of variation in timing of the peak flight periods that may be explained by all variables and the explanatory power of individual variables, respectively (e.g. Guisan and Zimmerman 2000). For this purpose, data were randomly divided into two sets in each five focal species: model fitting (70% of the data) and model validation (30%). This was done in order to allow for independent evaluation of model performance (i.e. predictive power). Predictive power was calculated here as the proportion of explained variance ( $r^2$ ) in the model testing part (30%) of the data (Guisan and Zimmerman 2000). Calculation of predictive power was done with models either excluding (i.e. producing an average prediction across sites by setting 'level = 0', see Pinheiro et al. 2014) or including site information as a random effect term. This was done in order to get an estimate of what proportion of the predictive power is due to the observational site and what proportion is due to the variation in the explanatory variable; with higher proportion of the latter expected to produce more reliable spatial predictions. This choice was done because calculation of an average prediction across large spatial scales is often more useful so that the general trend in phenology patterns will not be masked by local variation that is due to, for example, microclimatic factors. All LMMs were fitted as implemented in the nlme library, version 3.1-121 (Pinheiro et al. 2014) within the R statistical environment, version 3.2.2 (R Core Team, 2015).

### Producing spatial predictive maps of peak flight period

In order to produce spatial predictive maps of timing of the peak flight period for the focal species, we selected the total model including all variables and the single variable which showed reasonable predictive power ( $r^2 > 0.3$ ) in each respective species, that is, snow melt-off date in one species (*Orthosia gothica*) and vegetation greening date in another species (*Ectropis crepuscularia*) (Table 2). Spatial predictions were derived with the models excluding site information (Table S2), as described above. Maps showing the spatial distribution of the peak flight date in Finland were produced for the average period 2001–2013, an example year for an early peak flying period (2007) and an example late year (2006), chosen on the basis of a high and a low March–May mean temperature, respectively. In addition, an average prediction for 2001–2013 based on weekly accumulating thermal sum (i.e. GDD index with summation period starting on 1 January) was produced for both species. Thus, seven prediction maps are presented for both species.

To produce maps based on all variables, the input datasets were re-sampled to a common latitude–longitude grid at a spatial resolution of  $0.05 \times 0.05$  degrees. The

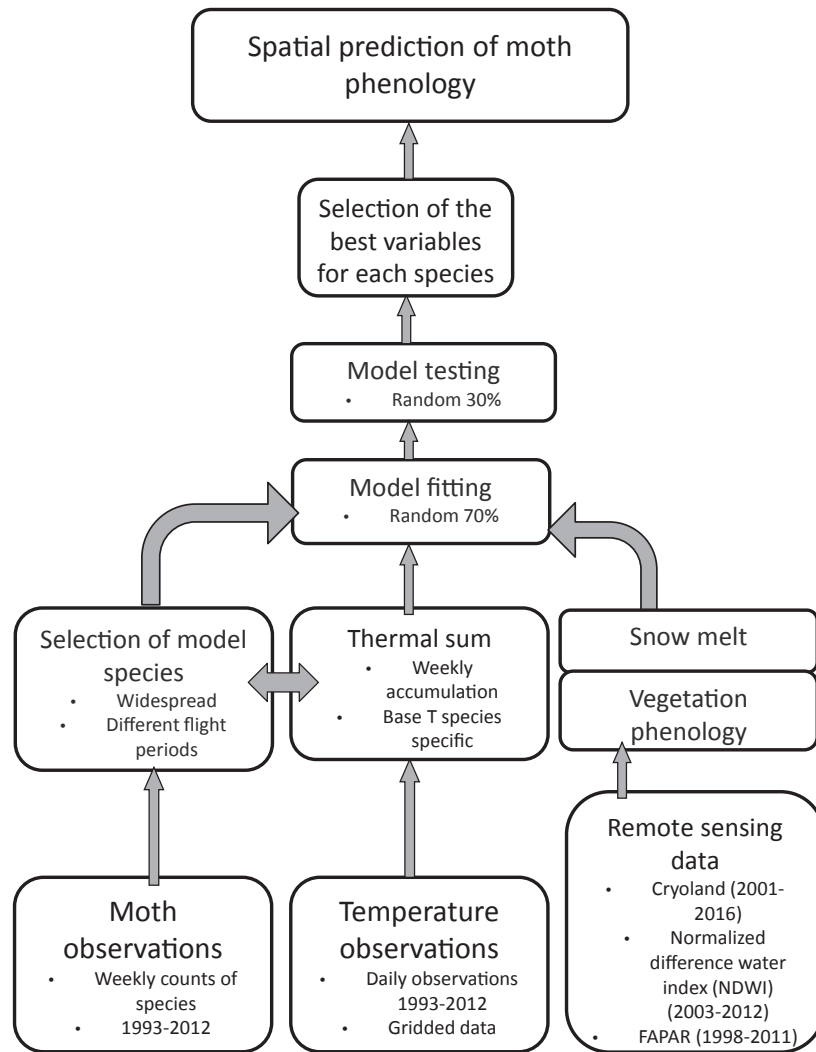


**Figure 2.** Flowchart of datasets used and analysis steps conducted for deriving predictive models of moth phenology.

maps of the greening date were smoothed and gap filled with a median filter with a kernel size of  $3 \times 3$  pixels prior to the application of the multivariate model. For FSGS the mean of the period 2001–2011 was used for the calculation of the average prediction maps for 2001–2013. Selection of the GDD index is explained above (see the section ‘Comparing predictive power of different variables’). Peak flight dates were transformed into periods of 5 days in length to facilitate drawing the maps.

## Results

### Comparison of variables

The predictive power ( $r^2$ ) of total LMMs (i.e. models including all corresponding explanatory variables)

calculated for the five focal species varied between 0.05 and 0.60 when site information was excluded and between 0.14 and 0.69 when site information was included (Table 2, Fig. S4). In univariate LMMs there was large variation in predictive power between species and variables but in most cases predictive power decreased markedly when site information was excluded (Table 2, Fig. 3, Fig. S4). In the early spring species (*Orthosia gothica*) snow melt-off date showed the highest predictive power that was retained after exclusion of site information (from  $r^2 = 0.68$  to  $r^2 = 0.59$ ) (Fig. 3A). Peak flight of the late spring species (*Ectropis crepuscularia*; Fig. 3B) was associated equally strongly with GDD and the greening date of vegetation ( $r^2 = 0.34$ , site information excluded), whereas in the late autumn species (*Operophtera brumata*, Fig. 3E), the strongest predictor of the peak

**Table 2.** Predictive power ( $r^2$ ) of linear mixed effect models (LMM) for the peak flight date in the randomly selected validation part (30%) of the data.

Species	Total model (all variables)	Latitude (Lat)	Weekly accumulating growing degree days (GDD)	Snow melt date (SMD)	Greening date (GD)	FAPAR start of growing season (FSGS)	FAPAR maximum date (FMD)	FAPAR end of growing season (FEGS)
<i>Orthosia gothica</i>	0.60 <sup>1</sup> (0.69 <sup>1</sup> )	0.38 (0.58)	0.42 <sup>1</sup> (0.60 <sup>1</sup> )	0.59 (0.68)	0.38 (0.58)	0.05 (0.54)	—	—
<i>Ectropis crepuscularia</i>	0.46 <sup>2</sup> (0.46 <sup>2</sup> )	0.17 (0.12)	0.34 <sup>2</sup> (0.31 <sup>2</sup> )	0.19 (0.19)	0.34 (0.39)	0.00 (0.05)	—	—
<i>Cabera exanthemata</i>	0.05 <sup>3</sup> (0.14 <sup>3</sup> )	0.05 (0.19)	0.01 <sup>3</sup> (0.12 <sup>3</sup> )	—	0.03 (0.18)	0.01 (0.13)	0.00 (0.16)	—
<i>Dysstroma citrata</i>	0.07 <sup>4</sup> (0.27 <sup>4</sup> )	0.00 (0.15)	0.03 <sup>4</sup> (0.27 <sup>4</sup> )	—	—	—	0.01 (0.20)	0.00 (0.19)
<i>Operophtera brumata</i>	0.48 <sup>5</sup> (0.56 <sup>5</sup> )	0.51 (0.57)	0.04 <sup>5</sup> (0.55 <sup>5</sup> )	—	—	—	0.01 (0.56)	0.01 (0.55)

The weekly accumulating GDDs depict the base threshold temperature ( $T_b$ ) used in the calculation as well as the date (DOY) that was selected for model calibration on the basis of Akaike Information Criterion (AIC) (see the superscripts). Predictive power is calculated for models both by excluding (i.e. by producing predictions averaged across sites) and by including site information (as a random effect term, in brackets). — indicates that the variable was not included in the respective model.

Weekly accumulating GDD parameters:

<sup>1</sup>Base temperature ( $T_b$ ) =  $-5^\circ\text{C}$ , summation period day-of-the-year (DOY) = 1–210.

<sup>2</sup> $T_b = 9^\circ\text{C}$ , DOY = 1–133.

<sup>3</sup> $T_b = 10^\circ\text{C}$ , DOY = 1–133.

<sup>4</sup> $T_b = 10^\circ\text{C}$ , DOY = 1–210.

<sup>5</sup> $T_b = 6^\circ\text{C}$ , DOY = 1–112.

flight was latitude ( $r^2 = 0.51$ , site information excluded). Peak flight periods of the mid and late summer species (*Cabera exanthemata*, *Dysstroma citrata*, Fig. 3C–D) were only weakly associated with the inspected explanatory variables ( $r^2 < 0.1$ , site information excluded).

### Spatial predictive models

Spatial prediction maps were produced for the two species (*Orthosia gothica* and *Ectropis crepuscularia*) for which remote sensing variables and GDD showed meaningful predictive power (Figs. 4 and 5). Separate predictions are presented for a total model including all variables, a model including one remote sensing variable with the highest predictive power (snow melt-off date in *Orthosia* (Fig. 4) and vegetation greening date in *Ectropis* (Fig. 5)) and a model based on an alternative variable (GDD). Under each model, example predictions are given for an average period of 2001–2013, a phenologically late year (2006) and a phenologically early year (2007). For the alternative variable (GDD) model, only an average prediction of 2001–2013 is given.

In *Orthosia gothica*, the peak flight starts on 25–29 April in south-western Finland and shifts by 20–24 May to the northernmost part of the country according to average predictions for the period 2001–2013 (Fig. 4A, D,

G). In an early example year (2007) the predicted peak flight occurred already on 15–19 April in south-western Finland (Fig. 4C and F), whereas in a late year (2006) the peak flight period was postponed to 30 April–4 May in the south of the country (Fig. 4B, E). However, in 2006 the latitudinal shift in timing of the peak flight period occurred faster than in 2007. In general, models based on all variables (Fig. 4A–C) and models based on a single variable (Fig. 4D–G) produced qualitatively similar spatiotemporal gradients for the occurrence of the peak flight period of *O. gothica*.

In *Ectropis crepuscularia*, the peak flight starts on 15–19 May in south-western Finland and shifts by 30 May–3 June to the northernmost part of the species range according to average predictions for the period 2001–2013 (Fig. 5A, D, G). In an early example year (2007) the predicted peak flight occurred on 10–14 May in southern Finland (Fig. 5C, F), whereas in a late year (2006) the peak flight period was postponed to 20–24 May in southern Finland but occurred then by 25–29 May across the entire distributional range in Finland (Fig. 5B, E). In contrast to *O. gothica*, in *E. crepuscularia* models based on all variables (Fig. 5A–C) predicted longer spatiotemporal gradients for the occurrence of the peak flight period than did models based on a single variable (Fig. 5D–G).

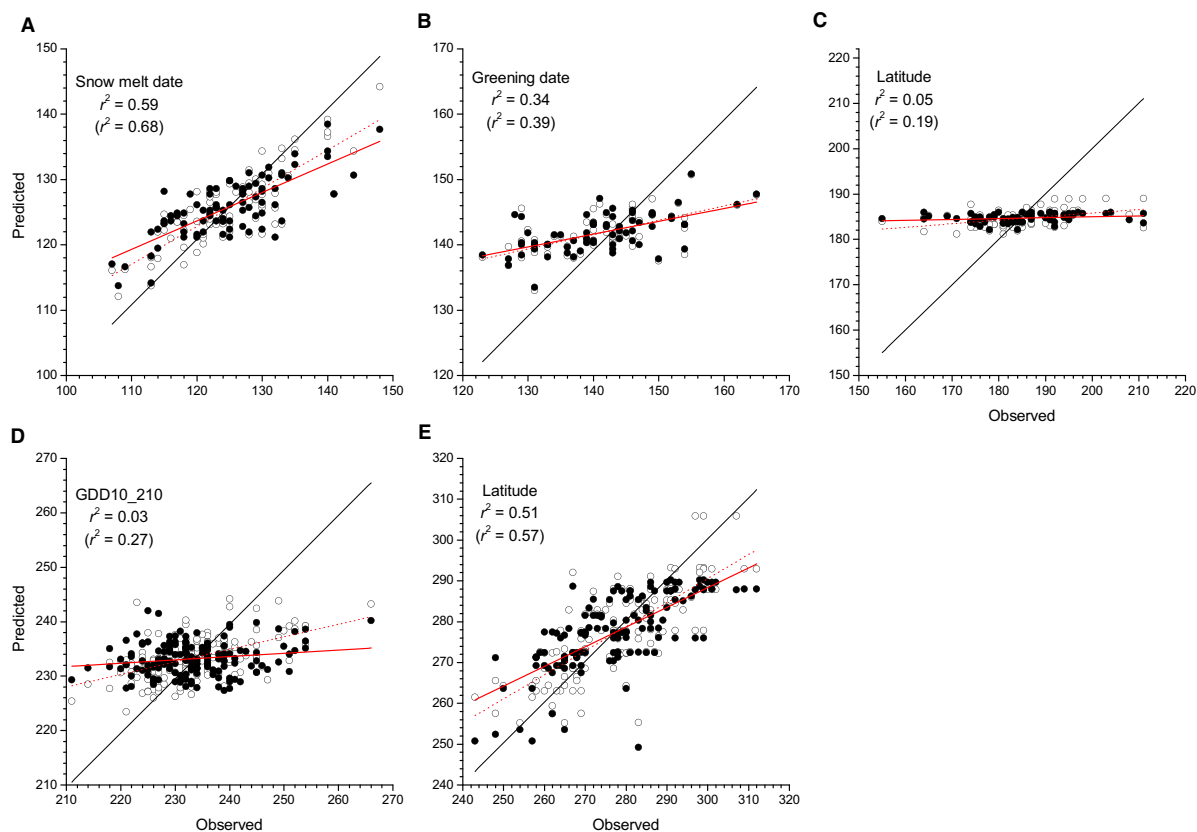


**Figure 3.** Predictive power of linear mixed effect models (LMM) including the single explanatory variable that showed the highest  $r^2$  value in the randomly selected 30% of the data across the five focal species: (A) *Orthosia gothica*, (B) *Ectropis crepuscularia*, (C) *Cabera exanthemata*, (D) *Dysstroma citrata* and (E) *Operophtera brumata*. All panels show dots for observed versus predicted values of peak flight dates, with black dots excluding (i.e. average prediction where level = 0) and open dots including site location in predictions. Red solid lines and dotted lines depict the model fits when site location is excluded (upper  $r^2$  value) and included ( $r^2$  value in parentheses), respectively, and black line depicts the identity line  $y = x$ .

## Discussion

The feasibility of remote sensing data in modelling and predicting phenology of animal species has received only little attention (cf. Roy et al. 2001; Nietschke et al. 2007; Hodgson et al. 2011). This is surprising considering that such methods are potentially very useful in the field of applied ecological sciences, including management of natural resources (White and Nemani 2006). Previously, earth observation products have been used to detect forest defoliations caused by pest species such as gypsy moth (*Lymantria dispar*; de Beurs and Townsend 2008; Spruce et al. 2011; Foster et al. 2013) and autumnal moth (*Epirrita autumnata*; Jepsen et al. 2009a; Babst et al. 2010; Olsson et al. 2016). Based on similar methodology, Trierweiler et al. (2013) and Sweet et al. (2015) developed NDVI-based models predicting overall temporal abundance of canopy arthropod biomass of grasshoppers and defoliation of birch trees, respectively, but they did not attempt predicting phenology of individual species. With

our work, we provide first tools towards a more widespread application of remote sensing datasets in modelling phenology of heterotrophic animal species and producing practical applications of spatial predictions.

According to our results, predictive ability of different variables is strongly affected by species identity. Notably, only in the species flying in early spring (*Orthosia gothica*) and late spring (*Ectropis crepuscularia*), remote sensing variables show good predictive power. In the three other species, however, none of the temperature-derived (i.e. thermal sum) and remote sensing variables showed meaningful predictive power. This result indicates that remote sensing variables are more clearly correlated with phenological patterns of those species in which the flight period coincides with distinguishable natural events such as snow melt or vegetation greening, which can easily be observed using remote sensing techniques. Thus, flight periods of these species also show potential in monitoring the impacts of climate change. For species that have their activity period in other parts of the season, it may be

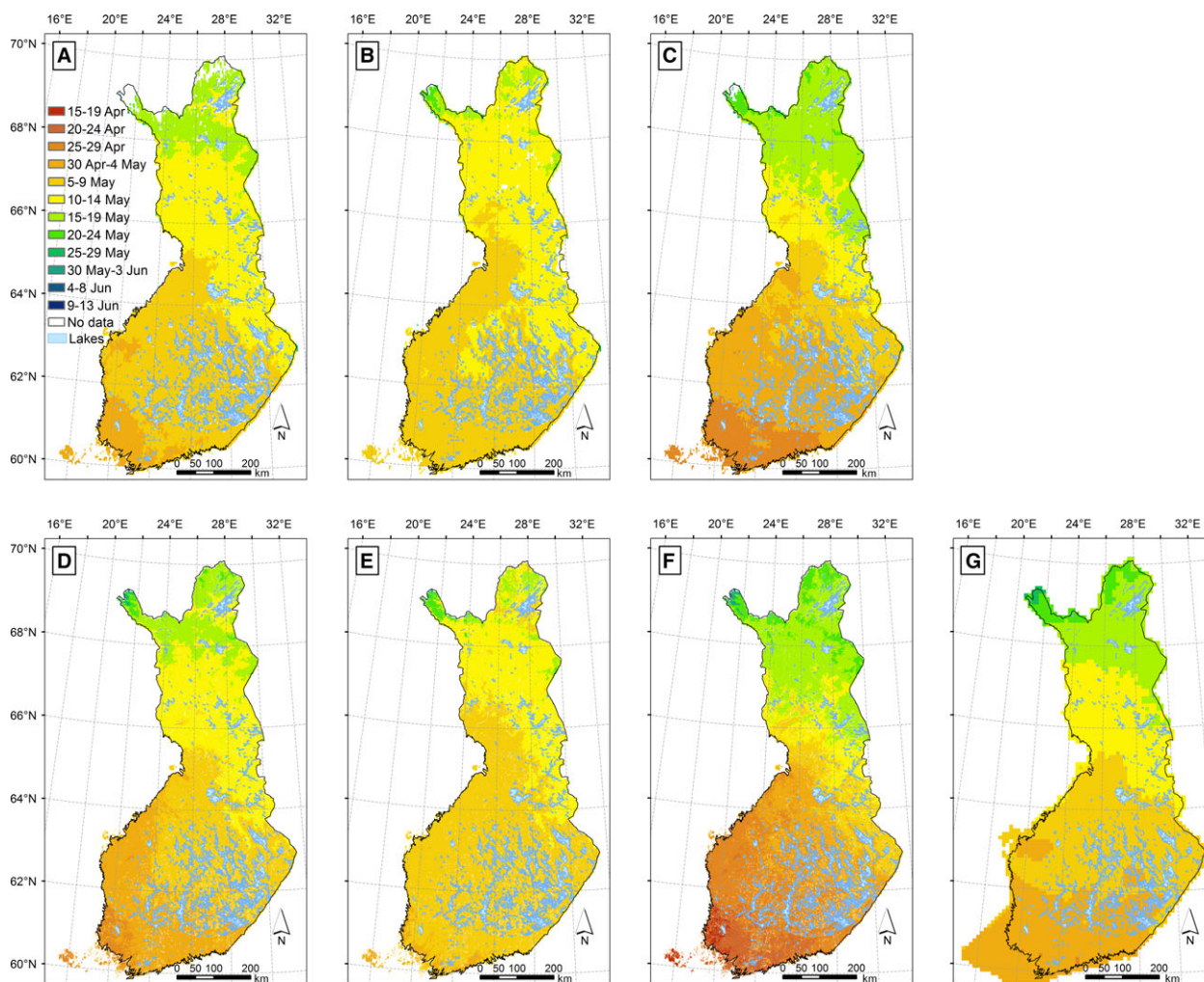


**Figure 4.** Maps of the peak flight periods for *Orthosia gothica*: predictions made on the basis of the total model including all variables for (A) an average period of 2001–2013, (B) a phenologically late year (2006), (C) a phenologically early year (2007); predictions made on the basis of snow melt-off date for (D) an average period of 2001–2013, (E) a phenologically late year (2006), (F) a phenologically early year (2007) and (G) an average prediction for 2001–2013 based on an alternative variable (weekly accumulating growing degree days). Model formulas are presented in Table S2. Data sources: Country borders © ESRI, Lakes © SYKE, Biogeographical provinces © LUOMUS and SYKE.

necessary to develop novel indicators based on remote sensing.

In general, it appears that predictive models do not fully describe the spatial gradient of moth peak flight. Model predictions generally showed a smaller range of values compared to observations, as can be seen by too late predictions of peak flight date for the south of Finland and too early predictions in northern Finland (Fig. 3, Fig. S4). Moreover, predictive power of the majority of investigated models decreased considerably after excluding the site information (represented as the random effect term) from the predictions (cf. Pinheiro et al. 2014). This indicates that the variables included in such models were not useful for making spatial predictions for the whole country, but instead their predictive

power was more closely related to the knowledge about exact locations of sites used in the model calibration. The choice of calculating an average prediction across large spatial scales was justifiable here because we were interested in the general trend in phenology patterns, which is not masked by local variation caused by, for example, microclimatic factors.

The predictive power of thermal sum, measured as GDD with varying base temperatures and summation periods, showed less variation across species when compared to remote sensing variables, but only when site information was included in spatial predictions. This indicates that temperature controls a large proportion of variation in timing of the flight period in these species, but this effect is also strongly dependent on local climatic variation. This is a

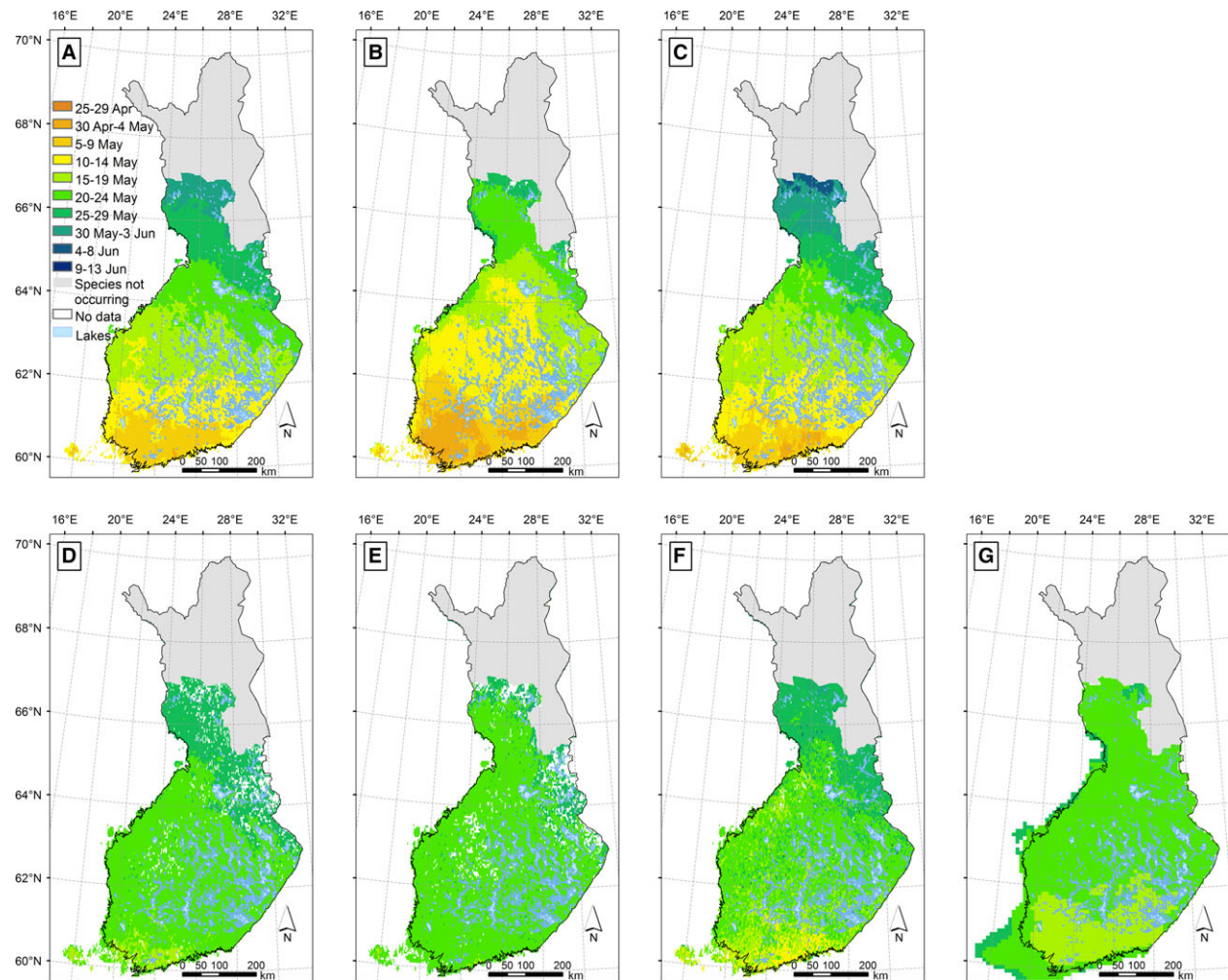


**Figure 5.** Maps of the peak flight periods for *Ectropis crepuscularia*: predictions made on the basis of the total model including all variables for (A) an average period of 2001–2013, (B) a phenologically late year (2006), (C) a phenologically early year (2007); predictions made on the basis of the vegetation greening date for (D) an average period of 2001–2013, (E) a phenologically late year (2006), (F) a phenologically early year (2007); and (G) an average prediction for 2001–2013 based on an alternative variable (weekly accumulating growing degree days). Model formulas are presented in Table S2. Data sources: Country borders © ESRI, Lakes © SYKE, Biogeographical provinces © LUOMUS and SYKE.

clear drawback in using temperature-derived variables in spatial predictions because large-scale spatial predictions are typically done without site information to avoid the general latitudinal trend being masked by the local variation. Previous studies have suggested that thermal controls determine timing of the flight period in a majority of moth species, and thus our results are only partly consistent with earlier studies (Valtonen et al. 2011, 2014).

The uncertainty of model predictions may stem from different sources, one of which being the differences in the temporal accuracy between the datasets deployed in the modelling, a factor that applies to both moth observational data and explanatory variables. The light traps used in collecting moth observational data are emptied usually once a week, but for logistic reasons there is some

additional variation in the length of the observational period. Thus, the temporal inaccuracy around the mid-day of the peak flight period calculated as average length of observational period divided by two varies between 3.67 and 4.26 days depending on the species identity. GDD indices defined with weekly varying summation periods were tested, but the spatial resolution (10 km × 10 km) and the representativeness of the underlying meteorological station network maybe too coarse to capture some of the microclimatic conditions at the trap sites. However, it is difficult to estimate this exactly. Onsite temperature observations made at the trap sites would probably increase predictive power of GDD indices, but such data were not available in this study. In the future, more fine-grained gridded temperature

products may become available and in part alleviate the shortcomings caused by too coarse scale of the gridded datasets.

By contrast, all the remote sensing datasets show an inherent temporal uncertainty. Snow melt and greening dates are estimated with the precision of 1 day, but in both cases missing observations stemming mainly from cloudiness cause some uncertainty that varies from year to year and by region depending on weather conditions. This is estimated to be ca. 5 days for snow melt date (Metsämäki et al. 2017), depending on the general snow cover conditions, that is, whether the area has a consistent seasonal snow cover or only sporadic snow occurrences. However, Metsämäki et al. (2017) demonstrate that compared with microwave data-based melt-off day information (which is not affected by such data gaps), the year-to-year trend of melt-off day is very similar. We can therefore expect that the inaccuracies obtained by using optical data such as MODIS do not have a remarkable effect on the results presented in this study. For the greening date, NDWI time series were interpolated at a daily time step and time series with a temporal gap larger than 2 weeks were discarded in the detection (Böttcher et al. 2016). The FAPAR dates for the start, maximum date and end of the growing season are obtained from 10-day products, and thus uncertainty is 5 days. Greening date and FAPAR growing season start date showed low correlation for the trap site locations in Finland (Table S1), although both satellite indices track the development of new foliage in the footprint of the satellite pixel. The satellite-based detection of the greening up of vegetation in Finland is challenging due to long periods of snow and cloud cover, fast vegetation development in spring and dominance of evergreen coniferous forest (e.g. Beck et al. 2006). The daily temporal resolution of the NDWI time series may be an advantage in this respect. Furthermore, the method for the greening date detection was targeted at and evaluated in boreal areas previously (see Delbart et al. 2006; Böttcher et al. 2016).

Data availability limits the applicability of using remote sensing variables when compared to temperature-derived variables. In the case of our work, all the remote sensing variables were available only for a part of the period (2003–2011) for which moth phenology data would be available (1993–2012). Although lack of datasets may be a major shortcoming in older time periods, the importance of this factor will diminish by time and continuing collection of data by satellites. The longer satellite data time series provided by TM (Thematic Mapper, 1984–2013) ETM+ (Enhanced Thematic Mapper Plus, 1999–present) and OLI (Operational Land Imager, 2013–present) on-board Landsat 5, Landsat 7 and Landsat 8, respectively, can be used in estimating the vegetation phenology and

with higher spatial resolution than moderate-resolution sensors such as MODIS. Despite the temporally sparse and spatially scarce nature of TM and ETM+ acquisitions, for example, a Bayesian approach introduced by Senf et al. (2017) maps the variation and temporal year-to-year changes in phenological events in a way that overcomes these deficiencies. Although their study was limited to a restricted area, such a technique is worth further investigation with longer phenological time series.

The impact of latitude was observed in the two species flying either in spring (*O. gothica*) or late autumn (*O. brumata*). This is not surprising as both species show a clear latitudinal gradient in timing of their peak flight period (Fig. S2). It has not been analysed how widespread latitudinal gradients in timing of the flight periods are in European moths, but in butterflies a majority of species show a shift towards later timing in the north (Roy and Asher 2003). However, it may be expected that moth species that have their flight season in the autumn will shift their flight period later towards the south (e.g. Pöyry et al. 2011).

The species sample included in this study was temporally representative, including one species flying at different times of the North European warm season, but yet quite limited in numbers. Thus, future studies focusing on a larger species set are required to verify the tentative observations made in this study. Moreover, previous studies have shown that in certain moth species, phenology is predominantly controlled by photoperiod (i.e. day length), or thermal controls are modified by photoperiod (see Valtonen et al. 2014). Although day length was included in models indirectly through latitude, it would be interesting to explore if predictive power of phenology models might be increased by accounting explicitly for photoperiod.

The spatial prediction methods demonstrated in this work allow for the prediction of timing of the peak flight periods of herbivorous insects, as exemplified here by moths, on the basis of both earth observation data and temperature observations. Such methodology has potential for application in other insect groups and extension to larger geographical areas. This enables also effective use of remote sensing variables (snow melt, greening) over large geographic areas in explaining phenology, when species-specific characteristics such as timing of flight period are taken into account. There are also widespread practical applications, for example, in supporting the achievement of the Aichi targets of biodiversity conservation, one of which being the development of new methodologies for monitoring of phenology in terrestrial ecosystems (CBD, 2014) and the monitoring, prediction and management of populations of insect pest species (e.g. Olsson et al. 2016).

## Acknowledgements

This work was supported by the European Commission Framework Programme (FP) 7 via project CLIPC (Constructing Europe's Climate Information Portal, [www.clipc.eu](http://www.clipc.eu)) (grant no. 607418). The authors would like to thank ENVEO IT GmbH for processing and distribution of the CryoLand FSC dataset and Pentti Pirinen from the Finnish Meteorological Institute for providing gridded daily temperature data. Remote sensing data of the green-up date in Finland were produced in the EU LIFE+ project Monimet (Grant agreement LIFE12 ENV/FI000409). We thank Mikko Kervinen from the Finnish Environment Institute for processing of NDWI time series from MODIS observations.

## Data Accessibility

The data used in this study is placed on the Knowledge Network for Biocomplexity (KNB) digital repository Pöyry, J. et al. (2017) Moth phenology modelling data from Finland 1993–2012. *Knowledge Network for Biocomplexity*. <https://doi.org/10.5063/f1542kks>.

## References

- Aarvik, L., B. Å. Bengtsson, H. Elven, P. Iivinskis, U. Jürivete, O. Karsholt, et al. 2017. Nordic-Baltic checklist of Lepidoptera. *Norw. J. Entomol. Suppl.* **3**, 1–236.
- van Asch, M., L. Salis, L. J. M. Holleman, B. van Lith, and M. E. Visser. 2013. Evolutionary response of the egg hatching date of a herbivorous insect under climate change. *Nat. Clim. Chang.* **3**, 244–248.
- Babst, F., J. Esper, and E. Parlow. 2010. Landsat TM/ETM+ and tree-ring based assessment of spatiotemporal patterns of the autumnal moth (*Epirrita autumnata*) in northernmost Fennoscandia. *Remote Sens. Environ.* **114**, 637–646.
- Badeck, F.-W., A. Bondeau, K. Böttcher, D. Doktor, W. Lucht, J. Schaber, et al. 2004. Responses of spring phenology to climate change. *New Phytol.* **162**, 295–309.
- Beck, P. S. A., C. Atzberger, K. A. Høgda, B. Johansen, and A. K. Skidmore. 2006. Improved monitoring of vegetation dynamics at very high latitudes: a new method using MODIS NDVI. *Remote Sens. Environ.* **100**, 321–334.
- de Beurs, K. M., and P. A. Townsend. 2008. Estimating the effect of gypsy moth defoliation using MODIS. *Remote Sens. Environ.* **112**, 3983–3990.
- Böttcher, K., T. Markkanen, T. Thum, T. Aalto, M. Aurela, C. Reick, et al. 2016. Evaluating biosphere model estimates of the start of the vegetation active season in boreal forests by satellite observations. *Remote Sens.* **8**, 580.
- Burnham, K. B., and D. R. Anderson. 2002. *Model selection and multimodel inference. A practical information-theoretic approach*, 2nd ed. Springer, New York.
- CBD (Convention on Biological Diversity). 2014. *Earth observation for biodiversity monitoring: a review of current approaches and future opportunities for tracking progress towards the aichi biodiversity targets*. Pp 183. Secretariat of the Convention on Biological Diversity, Canada. Technical Series No. 72.
- Ceccherini, G., N. Gobron, and M. Robustelli. 2013a. Harmonization of FAPAR from SeaWiFS and MERIS instruments. *Remote Sens.* **5**, 3357–3376.
- Ceccherini, G., N. Gobron, M. Migliavacca, and M. Robustelli. 2013b. Long-term measurements of plant phenology over Europe derived from SeaWiFS and Meris. In: L. Ouweland (ed.) *Proceedings of the 2013 ESA Living Planet Symposium, 9-13 September 2013*, Edinburgh, UK. ESA, Noordwijk, The Netherlands, Issue SP-722, ISBN 978-92-9221-286-5.
- Ceccherini, G., N. Gobron, and M. Migliavacca. 2014. On the response of European vegetation phenology to hydroclimatic anomalies. *Remote Sens.* **6**, 3143–3169.
- Delbart, N., L. Kergoat, T. Le Toan, J. L'Hermitte, and G. Picard. 2005. Determination of phenological dates in boreal regions using normalized difference water index. *Remote Sens. Environ.* **97**, 26–38.
- Delbart, N., T. Le Toan, L. Kergoat, and V. Fedotova. 2006. Remote sensing of spring phenology in boreal regions: a free of snow-effect method using NOAA-AVHRR and SPOT-VGT data (1982–2004). *Remote Sens. Environ.* **101**, 52–62.
- Delbart, N., G. Picard, T. Le Toan, L. Kergoat, S. Quegan, I. A. N. Woodward, et al. 2008. Spring phenology in boreal Eurasia over a nearly century time scale. *Glob. Change Biol.* **14**, 603–614.
- Finnish Environment Institute. 2009. CLC2006 Finland. Final technical report. Available at: <http://www.syke.fi/download/noname/%7BC7C849EB-3F4D-42AE-9A94-5B8069FFDFFB%7D/37641> (accessed 14 June 2017)
- Foster, J. R., P. A. Townsend, and D. J. Mladenoff. 2013. Mapping asynchrony between gypsy moth egg-hatch and forest leaf-out: putting the phenological window hypothesis in a spatial context. *For. Ecol. Manage.* **287**, 67–76.
- Ganguly, S., M. A. Friedl, B. Tan, X. Zhang, and M. Verma. 2010. Land surface phenology from MODIS: characterization of the collection 5 global land cover dynamics product. *Remote Sens. Environ.* **114**, 1805–1816.
- Gobron, N., B. Pinty, M. Taberner, F. Mélin, M. M. Verstraete, and J. L. Widowski. 2006. Monitoring the photosynthetic activity of vegetation from remote sensing data. *Adv. Space Res.* **38**, 2196–2202.
- Gonsamo, A., and J. M. Chen. 2016. Circumpolar vegetation dynamics product for global change study. *Remote Sens. Environ.* **182**, 13–26.
- Guisan, A., and N. E. Zimmerman. 2000. Predictive habitat distribution models in ecology. *Ecol. Model.* **135**, 147–186.

- Hodgson, J. A., C. D. Thomas, T. H. Oliver, B. J. Anderson, T. M. Brereton, and E. E. Crone. 2011. Predicting insect phenology across space and time. *Glob. Change Biol.* **17**, 1289–1300.
- Ivits, E., M. Cherlet, G. Tóth, S. Sommer, W. Mehl, J. Vogt, et al. 2012. Combining satellite derived phenology with climate data for climate change impact assessment. *Global Planet. Change* **88–89**, 85–97.
- Jepsen, J. U., S. B. Hagen, K. A. Høgda, R. A. Ims, S. R. Karlsen, H. Tømmervik, et al. 2009a. Monitoring the spatio-temporal dynamics of geometrid moth outbreaks in birch forest using MODIS-NDVI data. *Remote Sens. Environ.* **113**, 1939–1947.
- Jepsen, J. U., S. B. Hagen, S.-R. Karlsen, and R. A. Ims. 2009b. Phase-dependent outbreak dynamics of geometrid moth linked to host plant phenology. *Proc. R. Soc. B: Biol. Sci.* **276**, 4119–4128.
- Jung, M., M. Verstraete, N. Gobron, M. Reichstein, D. Papale, A. Bondeau, et al. 2008. Diagnostic assessment of European gross primary production. *Glob. Change Biol.* **14**, 2349–2364.
- Karlsen, S. R., A. Elvebakk, K. A. Høgda, and B. Johansen. 2006. Satellite-based mapping of the growing season and bioclimatic zones in Fennoscandia. *Glob. Ecol. Biogeogr.* **15**, 416–430.
- Lausch, A., L. Bannehr, M. Beckmann, C. Boehm, H. Feilhauer, J. M. Hacker, et al. 2016. Linking Earth Observation and taxonomic, structural and functional biodiversity: local to ecosystem perspectives. *Ecol. Ind.* **70**, 317–339.
- Leinonen, R., J. Pöyry, G. Söderman, and L. Tuominen-Roto. 2016. Suomen yöperhosseuranta (Nocturna) 1993–2012 [The Finnish moth monitoring scheme (Nocturna) 1993–2012]. Suomen ympäristökeskuksen raportteja, 15/2016, 71 p.
- Leyequien, E., J. Verrelst, M. Slot, G. Schaepman-Strub, I. M. A. Heitkönig, and A. Skidmore. 2007. Capturing the fugitive: applying remote sensing to terrestrial animal distribution and diversity. *Int. J. Appl. Earth Obs. Geoinf.* **9**, 1–20.
- Liu, Y. Y., A. I. J. M. van Dijk, M. F. McCabe, J. P. Evans, and R. A. M. de Jeu. 2013. Global vegetation biomass change (1988–2008) and attribution to environmental and human drivers. *Glob. Ecol. Biogeogr.* **22**, 692–705.
- Metsämäki, S. J., S. T. Anttila, H. J. Markus, and J. M. Vepsäläinen. 2005. A feasible method for fractional snow cover mapping in boreal zone based on a reflectance model. *Remote Sens. Environ.* **95**, 77–95.
- Metsämäki, S., O.-P. Mattila, J. Pulliainen, K. Niemi, K. Luojus, and K. Böttcher. 2012. An optical reflectance model-based method for fractional snow cover mapping applicable to continental scale. *Remote Sens. Environ.* **123**, 508–521.
- Metsämäki, S. J., K. Böttcher, J. Pulliainen, K. Luojus, O. P. Mattila, C. Derksen, et al. 2017. The accuracy of snow melt-off day derived from optical and microwave radiometer data and the relationship of snow water equivalent and fractional snow cover - a study for Europe. In review.
- Moulin, S., L. Kergoat, N. Viovy, and G. Dedieu. 1997. Global-scale assessment of vegetation phenology using NOAA/AVHRR satellite measurements. *J. Clim.* **10**, 1154–1155.
- Myneni, R. B., C. D. Keeling, C. J. Tucker, G. Asrar, and R. R. Nemani. 1997. Increased plant growth in the northern high latitudes from 1981 to 1991. *Nature* **386**, 698–702.
- Nagler, T., G. Bippus, C. Schiller, S. Metsämäki, O.-P. Mattila, K. Luojus, et al. 2015. CryoLand - Copernicus Service Snow and Land Ice: Final Report. In p. 46
- Nietschke, B. S., R. D. Magarey, D. M. Borchert, D. D. Calvin, and E. Jones. 2007. A developmental database to support insect phenology models. *Crop Prot.* **26**, 1444–1448.
- O'Connor, B., C. Secades, J. Penner, R. Sonnenschein, A. Skidmore, N. D. Burgess, et al. 2015. Earth observation as a tool for tracking progress towards the Aichi Biodiversity Targets. *Remote Sens. Ecol. Conserv.* **1**, 19–28.
- Olsson, P.-O., J. Lindström, and L. Eklundh. 2016. Near real-time monitoring of insect induced defoliation in subalpine birch forests with MODIS derived NDVI. *Remote Sens. Environ.* **181**, 42–53.
- Pettorelli, N., S. Ryan, T. Mueller, N. Bunnefeld, B. Jedrzejska, M. Lima, et al. 2011. The normalized difference vegetation index (NDVI): unforeseen successes in animal ecology. *Clim. Res.* **46**, 15–27.
- Pettorelli, N., W. F. Laurance, T. G. O'Brien, M. Wegmann, H. Nagendra, and W. Turner. 2014. Satellite remote sensing for applied ecologists: opportunities and challenges. *J. Appl. Ecol.* **51**, 839–848.
- Pinheiro, J., D. Bates, S. DebRoy, and D. Sarkar, & R Core Team. 2014. nlme: Linear and Nonlinear Mixed Effects Models. R package, version 3.1-118.
- Pöyry, J., R. Leinonen, G. Söderman, M. Nieminen, R. K. Heikkinen, and T. R. Carter. 2011. Climate-induced increase of moth multivoltinism in boreal regions. *Glob. Ecol. Biogeogr.* **20**, 289–298.
- Pritchard, G., L. D. Harder, and R. A. Mutch. 1996. Development of aquatic insect eggs in relation to temperature and strategies for dealing with different thermal environments. *Biol. J. Lin. Soc.* **58**, 221–244.
- R Core Team. 2015. R: A language and environment for statistical computing. R Foundation for Statistical Computing.
- Rautiainen, M., and P. Lukes. 2015. Spectral contribution of understory to forest reflectance in a boreal site: an analysis of EO-1 Hyperion data. *Remote Sens. Environ.* **171**, 98–104.
- Rautiainen, M., M. Möttö, J. Heiskanen, A. Akujärvi, T. Majasalmi, and P. Stenberg. 2011. Seasonal reflectance dynamics of common understory types in a northern European boreal forest. *Remote Sens. Environ.* **115**, 3020–3028.
- Roy, D. B., and J. Asher. 2003. Spatial trends in the sighting dates of British butterflies. *Int. J. Biometeorol.* **47**, 188–192.

- Roy, D. B., and T. Sparks. 2000. Phenology of British butterflies and climate change. *Glob. Change Biol.* **6**, 407–416.
- Roy, D. B., P. Rothery, D. Moss, E. Pollard, and J. A. Thomas. 2001. Butterfly numbers and weather: predicting historical trends in abundance and the future effects of climate change. *J. Anim. Ecol.* **70**, 201–217.
- Running, S. W., R. R. Nemani, F. A. Heinsch, M. Zhao, M. Reeves, and H. Hashimoto. 2004. A Continuous Satellite-Derived Measure of Global Terrestrial Primary Production. *Bioscience* **54**, 547–560.
- Senf, C., D. Pflugmacher, M. Heurich, and T. Krueger. 2017. A Bayesian hierarchical model for estimating spatial and temporal variation in vegetation phenology from Landsat time series. *Remote Sens. Environ.* **194**, 155–160.
- Spruce, J. P., S. Sader, R. E. Ryan, J. Smoot, P. Kuper, K. Ross, et al. 2011. Assessment of MODIS NDVI time series data products for detecting forest defoliation by gypsy moth outbreaks. *Remote Sens. Environ.* **115**, 427–437.
- Sweet, S. K., A. Asmus, M. E. Rich, J. Wingfield, L. Gough, and N. T. Boelman. 2015. NDVI as a predictor of canopy arthropod biomass in the Alaskan arctic tundra. *Ecol. Appl.* **25**, 779–790.
- Trierweiler, C., W. C. Mullié, R. H. Drent, K.-M. Exo, J. Komdeur, F. Bairlein, et al. 2013. A Palaearctic migratory raptor species tracks shifting prey availability within its wintering range in the Sahel. *J. Anim. Ecol.* **82**, 107–120.
- Valtonen, A., M. P. Ayres, H. Roininen, J. Pöyry, and R. Leinonen. 2011. Environmental controls on the phenology of moths: predicting plasticity and constraint under climate change. *Oecologia* **165**, 237–248.
- Valtonen, A., R. Leinonen, J. Pöyry, H. Roininen, J. Tuomela, and M. P. Ayres. 2014. Is climate warming more consequential towards poles? The phenology of Lepidoptera in Finland. *Glob. Change Biol.* **20**, 16–27.
- Venables, W. N., and B. D. Ripley. 2002. *Modern Applied Statistics with S*, 4th ed.. Springer-Verlag, New York.
- Venäläinen, A., H. Tuomenvirta, P. Pirinen, and A. Drebs. 2005. A basic Finnish climate data set 1961–2000 — description and illustrations. *Finnish Meteorol. Inst. Rep.* **5**, 1–27.
- Verstraete, M. M., N. Gobron, O. Aussedat, M. Robustelli, B. Pinty, J.-L. Widlowski, et al. 2008. An automatic procedure to identify key vegetation phenology events using the JRC-FAPAR products. *Adv. Space Res.* **41**, 1773–1783.
- Vihervaara, P., A.-P. Auvinen, L. Mononen, M. Törmä, P. Ahlroth, S. Anttila, et al. 2017. How Essential Biodiversity Variables and remote sensing can help national biodiversity monitoring. *Glob. Ecol. Conserv.* **10**, 43–59.
- Vrieling, A., A. K. Skidmore, T. Wang, M. Meroni, B. J. Ens, K. Oosterbeek, et al. 2017. Spatially detailed retrievals of spring phenology from single-season high-resolution image time series. *Int. J. Appl. Earth Obs. Geoinf.* **59**, 19–30.
- White, M. A., and R. R. Nemani. 2006. Real-time monitoring and short-term forecasting of land surface phenology. *Remote Sens. Environ.* **104**, 43–49.
- White, M. A., K. M. De Beurs, K. Didan, D. W. Inouye, A. D. Richardson, O. P. Jensen, et al. 2009. Intercomparison, interpretation, and assessment of spring phenology in North America estimated from remote sensing for 1982–2006. *Glob. Change Biol.* **15**, 2335–2359.
- Zhang, X., B. Tan, & Y. Yu. 2014. Interannual variations and trends in global land surface phenology derived from enhanced vegetation index during 1982–2010. *Int. J. Biometeorol.* **58**, 547–564.
- Zhao, J. J., H. Y. Zhang, Z. X. Zhang, X. Y. Guo, X. D. Li, and C. Chen. 2015. Spatial and temporal changes in vegetation phenology at middle and high latitudes of the Northern Hemisphere over the past three decades. *Remote Sens.* **7**, 10973–10995.

## Supporting Information

Additional supporting information may be found online in the supporting information tab for this article.

**Figure S1.** Locations of the moth monitoring trap sites that produced the phenological observations used in building the models.

**Figure S2.** Latitudinal gradient in timing of the peak flight period across the five focal species.

**Figure S3.** Two examples of timing of the peak flight periods of the focal moth species, snow melt-off dates (SMD), vegetation greening dates and dates of start (FSGS), peak (MD) and end (EGS) of the growing season derived from the FAPAR data. Both examples are from the year 2007, and situated in southern (Espoo) and northern (Kolari) part of Finland.

**Figure S4.** Model predictive power across the five focal species and different sets of explanatory variables.

**Table S1.** Pearson correlation coefficients among the explanatory variables for each focal species.

**Table S2.** Linear mixed effect models (LMM) fitted using randomly selected 70% of the phenological data using different sets of explanatory variables for the five focal species.